Aalborg Universitet

AALBORG UNIVERSITY
DENMARK

Cooperative Frequency Control for Autonomous AC Microgrids

Shafiee, Qobad; Quintero, Juan Carlos Vasquez; Guerrero, Josep M.; Nasirian, Vahidreza ; Davoudi, Ali

Cooperative Frequency Control for Autonomous AC Microgrids

Qobad Shafiee
Juan C. Vasquez
Josep M. Guerrero
www.microgrids.et.aau.dk
Department of Energy Technology
Aalborg University, Aalborg, Denmark
qsh,juq,joz@et.aau.dk

Vahidreza Nasirian
Ali Davoudi
Electrical Engineering Department
The University of Texas at Arlington
Arlington, Texas, USA
vahidreza.nasirian@mavs.uta.edu
davoudi@uta.edu

Abstract— **Distributed secondary control strategies have been recently studied for frequency regulation in droop-based AC Microgrids. Unlike centralized secondary control, the distributed one might fail to provide frequency synchronization and proportional active power sharing simultaneously, due to having different control parameters. This paper introduces a cooperative algorithm that regulates the system frequency while maintaining the power sharing properties of droop control. Dynamic consensus protocol is used to estimate the average of normalized active powers in the entire MG. This estimation is then added to primary control, compensating the frequency drop caused by the droop mechanism. The proposed controller is fully distributed, meaning that each source exchange information with only its direct neighbors through a sparse communication network. This controller has a unique feature that it does not require measuring the system frequency as compared to the other presented methods. An ac Microgrid with four sources is used to verify the performance of the proposed control methodology.**

Index Terms—**AC Microgrids, distributed control, frequency control, secondary control.**

I. INTRODUCTION

Due to the rapid development of renewable energy sources, the concept of Microgrid continues to gain popularity in recent years [1]-[5]. According to the US Department of Energy (DOE), a Microgrid is a group of interconnected loads and distributed energy resources within clearly defined electrical boundaries that acts as a single controllable entity with respect to the grid and that connects and disconnects from such grid to enable it to operate in both grid-connected or "island" mode. To ensure successful operation of Microgrids and to address different control requirements, a hierarchical control structure is conventionally adapted [6], [7]. The decentralized primary control is accommodated locally with each source inside the Microgrid in order to stabilize the system voltage and frequency. The secondary control is often used to remove frequency and voltage deviation produced by of the primary level [8], [9], and to achieve some other control goals such as load power sharing [10] and harmonic/unbalance compensation [11]. The highest hierarchy, the tertiary control, is in charge of economical operation and manages optimal operation of Microgrid in both islanded and grid-connected modes [12].

Conventional secondary control is centralized, located in the Microgrid Central Controller (MGCC). As a centralized controller, it requires communication network with fully connectivity which adds complexity to the system and compromises its reliability. Moreover, it introduces a single-point-of-failure to the design, i.e., any failure in the secondary control renders the entire system inoperable.

As an alternative, distributed control architecture has attracted a lot of interests recently, as it provides easier scalability, simpler communication network, and improved reliability [13], [14]. This control strategy has been recently studied for several Microgrid applications, e.g., secondary control [14]-[18]. For the purpose of frequency synchronization, distributed secondary control methodology has been practiced in the literature based on different protocols; networked averaging method [9], consensus algorithms [15]-[17], and gossip algorithm [18].

Although the existing works guarantee frequency synchronization in AC Microgrids, they might diminish proportional active power sharing. These controllers may either have different control parameters or distinct initial values, which affect the proportional load power sharing provided by $P - \omega$ droop control. Moreover, all the existing secondary control methods require frequency measurement to be able to regulate the system frequency.

This paper proposes a cooperative control framework to ensure simultaneous frequency regulation and proportional active power sharing in ac Microgrids. Main features of the proposed control methodology are as follows:
- Each source carries an embedded secondary controller which produces a frequency correction term. This correction term is added to droop control in order to

restore the system frequency to the nominal value while maintaining the active power shared between the sources in proportional to their power rates.

- It uses dynamic consensus protocol to estimate the average normalized active power across the Microgrid by comparing local generation with the neighbors'. This way, primary control of the MG sources receives the same correction term which is an global average value.

- Unlike centralized secondary controller and the existing distributed ones, frequency measuring is not required.

- A sparse communication network is only required spanned across the Microgrid to exchange the information; each source only communicates with its neighbors. Loss of communication links and other impairments, e.g., delay or packet loss, do not affect system operation as long as the communication graph remains connected. The control strategy is scalable, and plug play feature is applicable.

II. PRELIMINARY OF COOPERATIVE CONTROL AND GRAPHS

Sources inside a Microgrid can be connected via a distributed network of communication. Using communication interface, the Microgrid will be able to employ higher control levels on the top of decentralized primary control. Such a cyber network can be represented by a graph, as shown in Fig. 1, where sources and communication links are represented by nodes and edges, respectively. This cyber network facilitates cooperation among agents (sources), where any agent is in contact with only a few other agents as its neighbors, and not with all other agents. This cooperative interaction of the neighbors on the cyber layer sets the ground for the cooperative control, which offers convergence of the control variables (on all nodes) to a global consensus, if the communication graph is properly designed.

The communication graph may form a directed graph (digraph) between multiple agents, which is usually represented as a set of nodes $\mathbf{V_G} = v_1^g, v_2^g, ..., v_N^g$ connected with a set of edges $\mathbf{E_G} \subset \mathbf{V_G} \times \mathbf{V_G}$ and an associated adjacency matrix $\mathbf{A_G} = \left[a_{ij} \right] \in \Box^{N \times N}$, where N is the number of nodes (sources). The Adjacency matrix $\mathbf{A_G}$ carries the communication weights, where $a_{ij} > 0$ if $(v_j^g, v_i^g) \in \mathbf{E_G}$ and $a_{ij} = 0$ otherwise. The communication gains, a_{ij}s, can be assumed as data transfer gains. This paper assumes a time-invariant adjacency matrix. $N_i = j \mid (v_j^g, v_i^g) \in \mathbf{E_G}$ denotes the set of all neighbors of the Node i. Equivalently, if $j \in N_i$, then v_i^g receives information from v_j^g. However, the links are not necessarily reciprocal, i.e., v_j^g may not receive information from v_i^g. The in-degree matrix $\mathbf{D_G^{in}} = \text{diag } d_i^{in}$ is a diagonal matrix with $d_i^{in} = \sum_{j \in N_i} a_{ij}$. Similarly, the out-degree matrix is $\mathbf{D_G^{out}} = \text{diag}\{d_i^{out}\}$, where $d_i^{out} = \sum_{i \in N_i} a_{ji}$. The Laplacian matrix is defined as $\mathbf{L} = \mathbf{D_G^{in}} - \mathbf{A_G}$, whose eigenvalues determine global dynamics of the system. The Laplacian matrix is balanced if the in-degree of each node matches its out-degree, i.e.,

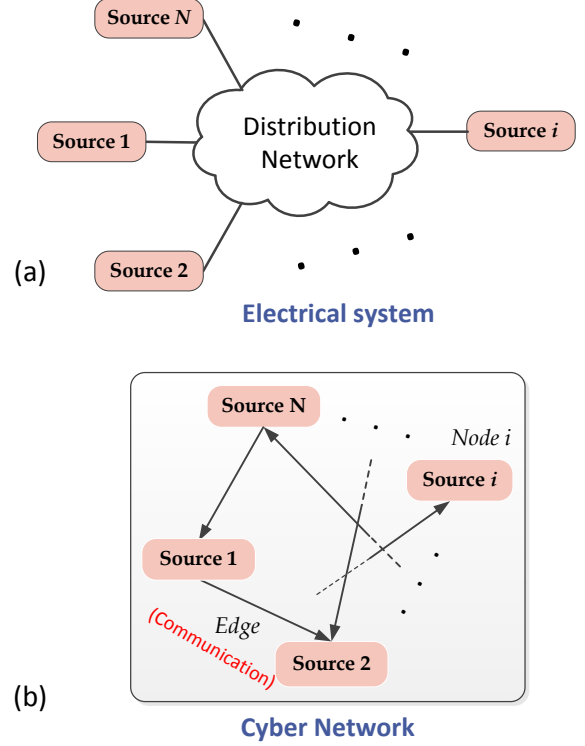(a) Electrical system

(b) Cyber Network

Figure 1. Layout of an AC Microgrid augmented with a communication network. (a) Electrical configuration of the Microgrid, (b) Graphical representation of the cyber network.

$\mathbf{D_G^{in}} = \mathbf{D_G^{out}}$. A direct path from v_i^g to v_j^g is a sequence of edges that connects the two nodes. A digraph is said to have a spanning tree if it contains a root node, from which there exists at least a direct path to every other node. Practically, the communication graph is chosen such that in case of any link failure the remaining network still contains at least one spanning tree.

III. PROPOSED COOPERATIVE FREQUENCY CONTROL FRAMEWORK

A distributed controller based on dynamic consensus protocol is proposed for frequency synchronization of AC Microgrids. In the proposed methodology, each source of Microgrid is equipped with a local frequency controller. These controllers are linked through a sparse communication network to facilitate data exchange. This cyber network can be directed or undirected (bidirectional) which has at least one spanning tree, with a balanced Laplacian matrix. Each source (controller), e.g., the source at Node i, relays an information, $\Psi_i = \left[\overline{p}_i^{norm} \right]$, to its neighbors on the graph, where $\overline{p}_i^{norm}$ is estimation of the averaged normalized active power at Node i. The normalized active power refers to the supplied active power by the source i, p_i, multiplied by its corresponding droop coefficient, m_i. Each controller receives data from its neighbors on graph and, through processing local and
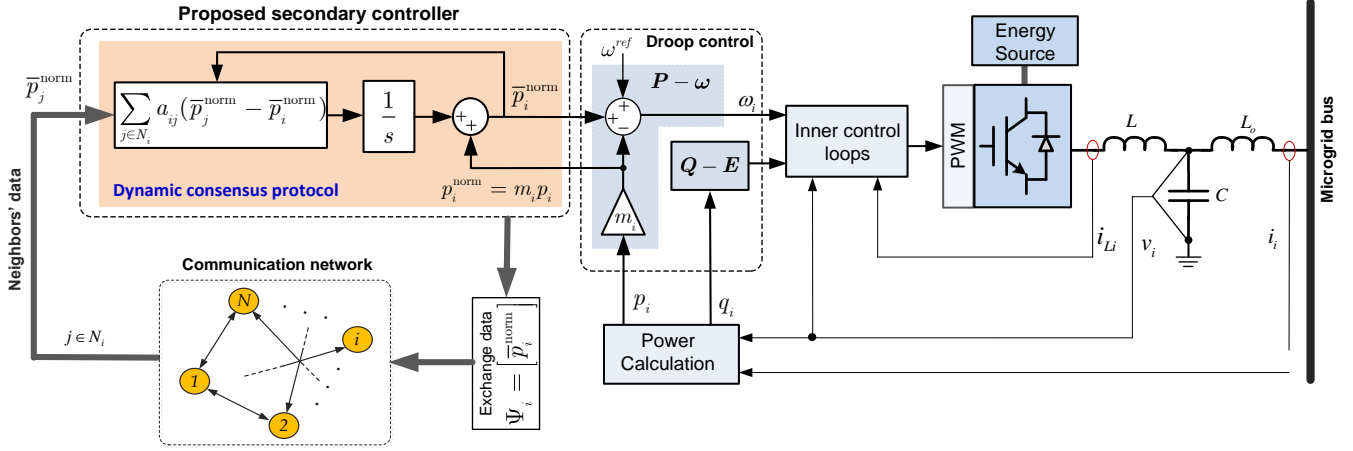
Figure 2. The proposed control methodology implemented at i-th source in an islanded ac Microgrid.

neighbors' information, it updates its control variables using a consensus protocol. The control signal is sent to primary droop control then to synchronize the frequency.

Figure 2 shows the proposed control methodology for an arbitrary source, e.g., source i. As Fig. 2 shows, the regulator at each node provides the estimated average of normalized active power, $\overline{p}_i^{\mathrm{norm}}$, across the Microgrid. This estimation is made using a distributed approach so-called *dynamic consensus* protocol [19], [20]. This average value is utilized as global signal to be added to droop control of sources. The distributed controller at Node i updates its average dynamically based on

$$\overline{p}_i^{\mathrm{norm}}(t) = p_i^{\mathrm{norm}}(t) + \int_0^t \sum_{j \in N_i} a_{ij} \left(\overline{p}_j^{\mathrm{norm}}(\tau) - \overline{p}_i^{\mathrm{norm}}(\tau) \right) \mathrm{d}\tau, \quad (1)$$

$$\overline{p}_i^{\mathrm{norm}}(t) = m_i p_i(t) \quad (2)$$

where p_i is the measured active power, $\overline{p}_j$ is the average normalized active power provided by the estimator at Node j which has direct communication with Node i. As seen in (1), the updating protocol uses the local normalized active power, p_i^{norm}, in order to consider the influence of active power variation in estimation process. It is shown in [19] that the dynamic consensus protocol will converge to a global consensus which is true average value of signals, if the communication graph is defined properly. Therefore, the estimated average normalized active power in each node is

$$\lim_{t \to \infty} \overline{p}_i^{norm}(t) = \frac{1}{N} \sum_{i=1}^N p_i^{norm}(t) = \frac{1}{N} \sum_{i=1}^N m_i p_i(t). \quad (3)$$

The average normalized active power produced by the consensus protocol in (1), act as a frequency correction term.

This term boosts frequency of all the sources successfully and accordingly synchronizes the system frequency. In addition, as the average normalized active powers, $\overline{p}_i^{\mathrm{norm}}$ s, converge to the same value in steady-state, the controller provides proportional active load sharing.

IV. RESULTS

A Microgrid test bench, shown in Fig. 3, includes four sources with various rated powers supplying local loads and distant loads, is considered to study performance of the control methodology. Rated power of the first two sources is twice those for the last two (see Table I). Rated voltage of the system is 230 V with the frequency of 50 Hz. LCL filters are installed at the inverters' outputs to reduce the harmonics caused by switching. Distribution line impedances are modeled with series RL branches. As highlighted in Fig. 3, the Microgrid is equipped with a communication network for data exchange between the distributed controllers. The links are all assumed to be bidirectional to maintain graphical connectivity in case of a link/inverter failure. The proposed control strategy is simulated in Matlab Simulink®. Associated adjacency matrix of the cyber network, $\mathbf{A_G}$, is

$$\mathbf{A_G} = 250 \times \begin{bmatrix} 0 & 1 & 0 & 1 \\ 1 & 0 & 1 & 0 \\ 0 & 1 & 0 & 1 \\ 1 & 0 & 1 & 0 \end{bmatrix}. \quad (4)$$

Other electrical and control parameters of the underlying system are tabulated in details in Table I. Subsequent studies evaluates performance of the proposed controller:
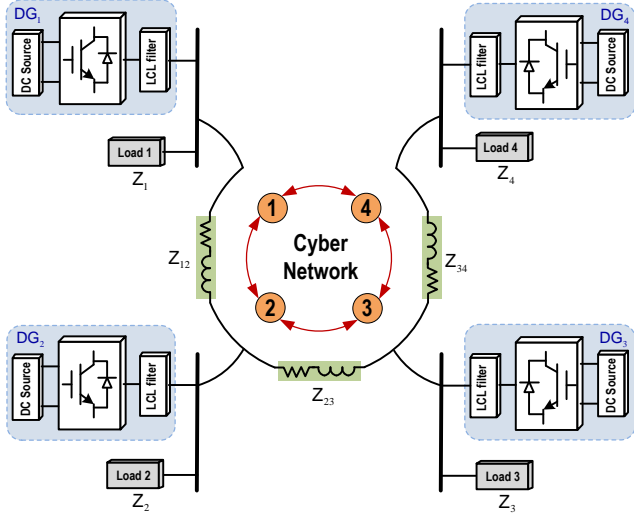
Figure 3. A Microgrid test bench facilitated with cyber network.

(a)

(b)

(c)

Figure 4. Performance of the proposed control methodology.

TABLE I

MICROGRID TEST BENCH ELECTRICAL AND CONTROL PARAMETERS

Electrical parameters		
Parameter	Symbol	Value
DC voltage	V_{dc}	650 V
MG voltage amplitude	e^{ref}	325 V
MG frequency	f	50 Hz
LCL filter capacitance	C	25 μF
LCL filter inductance	L	1.8 mH
LCL filter impedance	L_o	1.8 mH
Load 1, Load 2	Z_1 , Z_2	$300 + j314\ \Omega$
Load 3, Load 4	Z_3 , Z_4	$150 + j157\ \Omega$
Line impedance 1, 2	Z_{12}	$R_{12} = 1.2\ \Omega,\ L_{12} = 5.4$ mH
Line impedance 2, 3	Z_{23}	$R_{23} = 0.4\ \Omega,\ L_{23} = 1.8$ mH
Line impedance 3, 4	Z_{34}	$R_{34} = 0.4\ \Omega,\ L_{34} = 3.2$ mH
Control Parameters			
---	---	---	---
Symbol	Symbol	Sources 1&2	Sources 3&4
Rated active power	p_{max}	1600 W	800 W
Rated reactive power	q_{max}	600 VAr	300 VAr
$P - \omega$ droop coefficient	m	0.002	0.004
$Q - V$ droop coefficient	n	0.01	0.02

A. Proposed controller performance

Figure 4 evaluates performance of the proposed control framework. For $t < 16$ s conventional droop is effective, and then the proposed controller is activated at $t = 16$ s. Response of the controller to load change is studied afterward. When primary droop control is running, frequency deviation from the rated values can be observed in all the sources (see Fig. 4(a)), while active power is proportionally shared among the sources.

The system frequency is restored to the desired value after activating the controller at $t = 16$ s. It eliminates the frequency deviations caused by droop controllers quickly, and maintains the a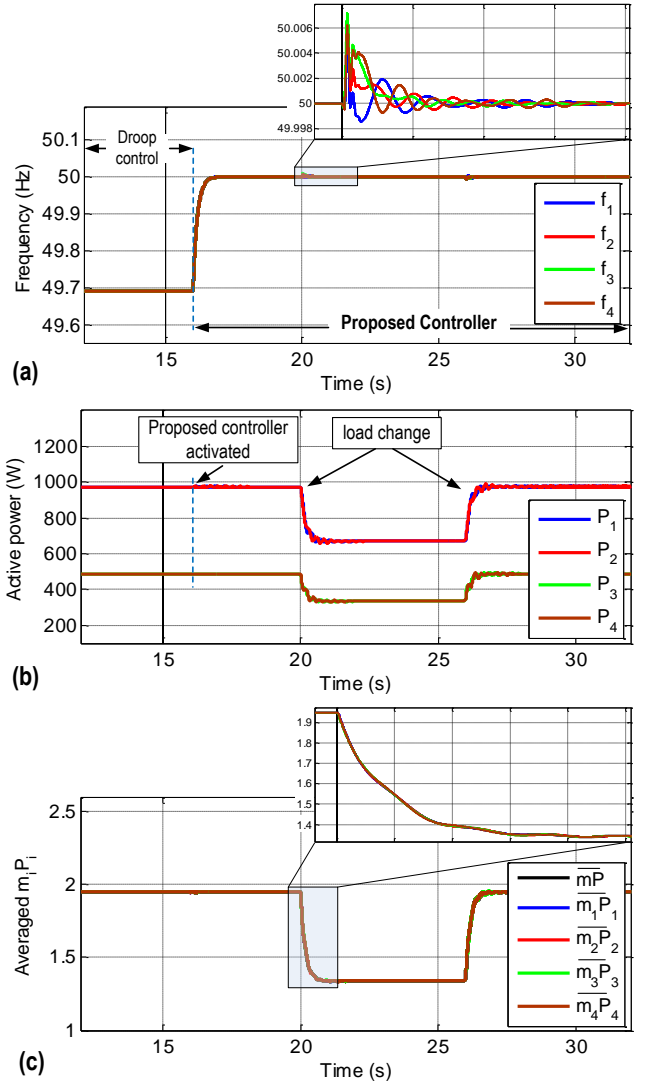ctive power proportionally shared among the sources. Estimated average of normalized active powers, $\bar{p}_i^{norm} = m_i p_i$s, are compared with the true average, $\bar{p}^{norm} = \frac{1}{N}\sum_{i=1}^{N} p_i^{norm}$, in Fig. 4(c), where results show the excellent match.[1] In fact, this estimation is the frequency correction term, as it is directly added to the droop mechanism (see Fig. 2). The results shows this fact that all the sources receive the same frequency correction term from the proposed controller which results in keeping active powers proportionally shared inside the system.

Controller response to step load changes is studied next. The local load at the third bus is unplugged at $t = 20$ s and plugged back in at $t = 26$ s. The results show that the proposed controller effectively synchronizes the system frequency and maintains the active power proportionally shared among the sources, even at the presence of large load disturbances.
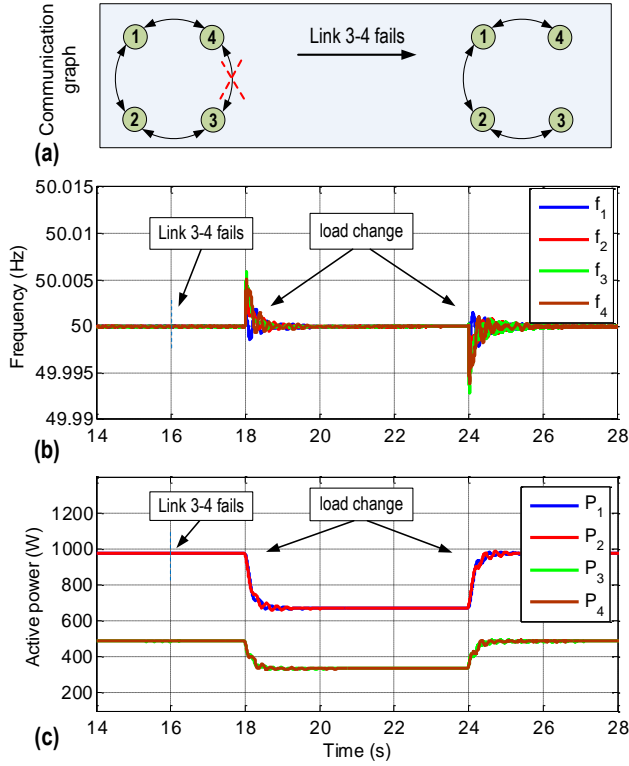
(a)

(b)

(c)

Figure 5. Communication link failure.

(a)

(b)

(c)

Figure 6. Plug-and-play capability

B. Resiliency to a communication link failure

As Fig. 3 shows, original communication graph is designed to carry a minimum redundancy, such that no single communication link failure can compromise the connectivity of the cyber network. To validate this, resiliency to a single link failure is studied in Fig. 5. The communication link between Source 3 and Source 4 is set to fail at $t = 16$ s. As seen in this figure, the link failure does not impact frequency synchronization or load sharing in the Microgrid. Indeed, no single link failure does hinder the graphical connectivity. This concept is illustrated in Fig. 5(a), where it is shown that the graph remains connected when the link 3-4 is disabled.

However, any loss of connection affects the Laplacian matrix and, thus, the system dynamic. To study that effect, a frequent step load change is practiced with the failed link. The load connected to Bus 3 (Z_3) has been unplugged and plugged back in at moments $t = 18$ s and $t = 24$ s. As results show, the frequency synchronization and proportional active power sharing are successfully carried out despite having a failed link in the system. Nevertheless, comparing active power signals in Fig. 4 and Fig. 5 implies that the system dynamic has slightly slowed down in Fig. 5 due to the loss of a communication link.

Similarly, performance of the controller at the presence of different cyber network topologies, as well as different failed link can be examined.
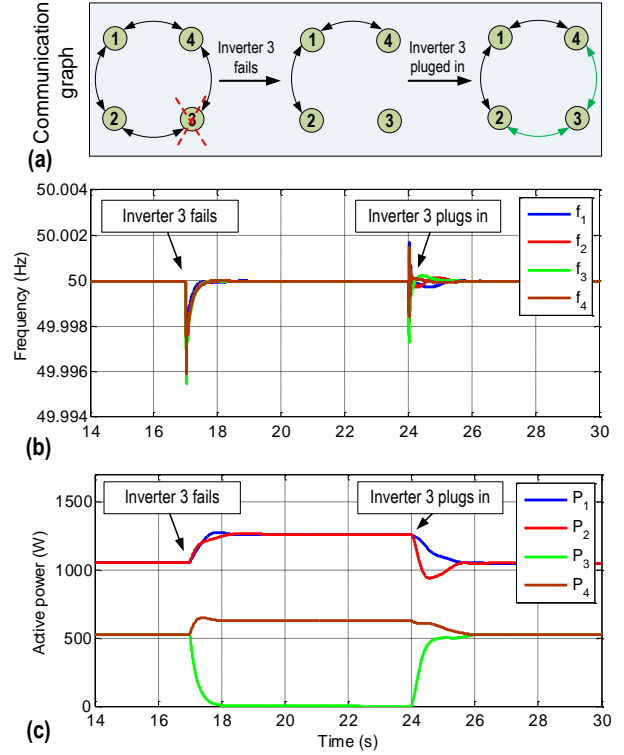
C. Plug and Play Capability

Plug-and-play capability, as a common contingency in Microgrids, is subjected to study next. Figure 6 illustrates how the proposed controller behaves when a source enters/leaves the Microgrid. Inverter 3 is intentionally disconnected from the Microgrid at $t = 17$ s to mimic loss of a source, and connected back again at $t = 24$ s. In practice, loss of a source also means the loss of all communication links attached to that particular source. The communication graph has been designed to remain connected in case of a source failure. After failure of links 2-3 and 3-4 due to loss of inverter 3, the existing links still form a connected graph (see Fig. 6(a), thus, the controller is expected to remain operational. When the third inverter is disconnected at $t = 17$ s, the frequency synchronization is still preserved and the excess active power is proportionally shared among the remaining sources.

A synchronization process has been applied to synchronize the inverter 3 with the Microgrid and to regulate its frequency and voltage before connection. After successful synchronization, inverter 3 is reconnected to the Microgrid at $t = 24$ s. As Figure 6 indicates that the proposed control methodology maintains accurate proportional power sharing and synchronizes the system frequency successfully when a new source enters/leaves the Microgrid.

V. Conclusion

A cooperative control framework is introduced that handles simultaneous frequency synchronization and proportional active power sharing in AC Microgrids. The controller compares the local normalized active power with the neighbors' and, accordingly, adjusts the frequency (or, phase angle) set point to carry out the proportional active power sharing. The proposed method only requires sparse communication network to exchange data. Unlike the existing centralized and distributed methods, no frequency measurement is needed for regulating the system frequency. Simulation studies show effectiveness of the proposed controller under different studies: load change, resiliency to a single communication link failure, and plug-and-play capability.

References

[1] F. Katiraei, R. Iravani, N. Hatziargyriou, and A. Dimeas, "Microgrids management", *IEEE Power Energy Mag.*, vol. 6, no. 3, pp. 54–65, 2008.

[2] J. A. P. Lopes, C. L. Moreira, and A. G. Madureira, "Defining control strategies for Microgrids islanded operation," *IEEE Trans. Power Syst.*, vol. 21, pp. 916–924, May 2006.

[3] E. Serban and H. Serban, "A control strategy for a distributed power generation microgrid application with voltage- and current-controlled source converter," *IEEE Trans. Power Electron.*, vol. 15, pp. 2981–2992, Dec. 2010.

[4] J. Rocabert, A. Luna, F. Blaabjerg, and P. Rodriguez, "Control of power converters in ac microgrids," *IEEE Trans. Power Electron.*, vol. 27, pp. 4734–4749, Nov. 2012.

[5] J. Hu, J. Zhu, D. G. Dorrell, and J. M. Guerrero, "Virtual flux droop method – A new control strategy of inverters in microgrids," *IEEE Trans. Power Electron.*, vol. 29, pp. 4704–4711, Sept. 2014.

[6] J. M. Guerrero, M. Chandorkar, T. Lee, and P. C. Loh, "Advanced control architectures for intelligent microgrids—part I: Decentralized and hierarchical control," *IEEE Trans. Ind. Electron.*, vol. 60, no. 4, pp. 1254–1262, April 2013.

[7] A. Bidram and A. Davoudi, "Hierarchical structure of Microgird control system," *IEEE Trans. Smart Grid*, vol. 3, no. 4, pp. 1963–1976, Dec. 2012.

[8] A. Bidram, A. Davoudi, F. L. Lewis, and J. M. Guerrero, "Distributed cooperative secondary control of Microgrids using feedback linearization," *IEEE Trans. Power Syst.* vol. 28, no. 3, pp. 3462–3470, Aug. 2013.

[9] Q. Shafiee, J. M. Guerrero, and J. C. Vasquez, "Distributed secondary control for islanded microgrids – A novel approach," *IEEE Trans. Power Electron.*, vol. 29, pp. 1018–1031, Feb. 2014.

[10] A. Micallef, M. Apap, C. Spiteri-Staines, J. M. Guerrero, and J. C. Vasquez, "Reactive power sharing and voltage harmonic distortion compensation of droop controlled single phase islanded microgrids," *IEEE Trans. Smart Grid*, vol. 5, pp. 1149-1158, May 2014.

[11] L. Meng, X. Zhao, F. Tang, M. Savaghebi, T. Dragicevic, J. C. Vasquez, J. M. Guerrero, "Distributed voltage unbalance compensation in islanded Microgrids by using dynamic-consensus-algorithm," *IEEE Trans. Power Electron.*, Early Access.

[12] L. Meng, F. Tang, M. Savaghebi, J. C. Vasquez, J. M. Guerrero, "Tertiary Control of Voltage Unbalance Compensation for Optimal Power Quality in Islanded Microgrids," IEEE Trans. *Energy Convers.*, vol.29, no.4, pp.802–815, Dec. 2014.

[13] H. Liang, B. J. Choi, W. Zhuang, X. Shen, A. S. A. Awad, and A. Abdr, "Multiagent coordination in microgrids via wireless networks," *IEEE Wireless Commun.*, vol. 19, pp. 14_22, June 2012.

[14] V. Nasirian, A. Davoudi, F. L. Lewis, and J. M. Guerero, "Distributed Adaptive Droop Control for DC Distribution Systems," *IEEE Trans. Energy Convers.*, vol.29, no.4, pp.944–956, Dec. 2014.

[15] J. W. Simpson-Porco, F. Dorfler, and F. Bullo, "Synchronization and power sharing for droop-controlled inverters in islanded Microgrids," *Automatica*, vol. 49, no. 9, pp. 2603–2611, Sept. 2013.

[16] Q. Shafiee, V. Nasirian, J. M. Guerrero, F. L. Lewis, A. Davoudi "Team-oriented Adaptive Droop Control for Autonomous AC Microgrids," in *Proc. 40th annu. Conf. IEEE Ind. Electron. Soc. (IECON)*, Oct. 2014.

[17] A. Bidram, A. Davoudi, and F. L. Lewis, "A multi-objective distributed control framework for islanded microgrids," *IEEE Trans. Ind. Informatics*, vol. 10, no. 3, pp. 1785–1798, Aug. 2014.

[18] Q. Shafiee, T. Dragicevic, J. C. Vasquez, and J. M. Guerrero, C. Stefanovic, P. Popovski, "A novel robust communication algorithm for distributed secondary control of islanded MicroGrids," in *Proc. IEEE Energy Convers. Cong. Expo. (ECCE)*, Sept. 2013, pp.4609–4616.

[19] R. Olfati-Saber and R. M. Murray, "Consensus problems in networks of agents with switching topology and time-delays," *IEEE Trans. Autom. Control*, vol. 49, no. 9, pp. 1520–1533, 2004.

[20] D. P. Spanos, R. Olfati-Saber, and R. M. Murrary, "Dynamic consensus for mobile network," in *Proc. 16th Int. Fed. Aut. Control (IFAC)*, 2005, pp. 1–6.